

Cytotoxicity of *Zingiber officinale* var. *rubrum* on HeLa cells and prediction of anti-proliferative activity via the JAK2/STAT3 and hedgehog pathways using a molecular docking approach

Siti Rofida^{1,2}, Laela Hayu Nurani^{2*}, Dwi Utami², Citra Ariani Edityaningrum²

¹Faculty of Health Science, University of Muhammadiyah Malang, Malang,
Jl. Bandung No. 1 Malang, East Java, Indonesia

²Faculty of Pharmacy, Universitas Ahmad Dahlan
Jl. Prof. Dr. Soepomo, S.H., Warungboto, Umbulharjo, Yogyakarta, Indonesia

Submitted: 31-10-2023

Reviewed: 16-12-2023

Accepted: 29-12-2023

ABSTRACT

Cervical cancer is one of the second-leading causes of death in women. The discovery of cancer drug candidates continues to be carried out due to the resistance that occurs in cervical cancer therapy. Plant metabolite compounds are one of the sources used to explore new drug candidates. Red ginger rhizome is a candidate plant that has anti-cervical cancer activity. This study aims to determine the cytotoxicity of an ethanol extract of red ginger rhizomes on the growth of HeLa cancer cells and predict anti-proliferative activity via the JAK2/STAT3 and hedgehog pathways. The sample (red ginger rhizome simplicia) was extracted by remaceration using 75% ethanol. The MTT assay method was used to test the cytotoxicity and anti-proliferation of metabolite compounds. The docking molecular study was performed by using Autodock 4.2.6.6.5 software. The receptors used in the JAK2, STAT3, and SMO pathways were obtained from the Protein Data Bank with the codes 6VGL, 6NUQ, and 5L7I, respectively. The ethanol extract produced a thick yellowish-brown extract with an aromatic smell and spicy taste, with an extract yield of 18.63% w/w. The 75% ethanol extract of red ginger rhizomes had cytotoxic activity in HeLa cancer with an IC_{50} of 104.22 ± 6.18 μ g/mL and an IC_{50} of cisplatin of 38.61 ± 3.66 μ g/mL. Prediction of antiproliferative activity via the JAK2 pathway showed a binding energy and K_i value of -7.47 kcal/mol, -7.48 kcal/mol, and 3.33 μ M, 3.27 μ M, as shown by alpha-cedrol and beta-eudesmol compounds. The highest inhibition on the STAT3 and SMO pathways was shown by the beta compound eudesmol, with binding energy and K_i values of -6.05 kcal/mol, -7.57 kcal/mol, and 36.48 μ M, respectively; 2.81 μ M. (provide relevance and implication)

Keywords: cancer, cervix, docking, red ginger rhizome, IC_{50}

*Corresponding author:

Laela Hayu Nurani

Department of Biology Pharmacy, Faculty of Pharmacy, Universitas Ahmad Dahlan

Jl. Prof. Dr. Soepomo, S.H., Warungboto, Umbulharjo, Yogyakarta, Indonesia

Email: laela.farmasi@pharm.uad.ac.id



INTRODUCTION

Cervical cancer is the second biggest cause of mortality in women after heart disease. According to WHO estimates, cervical cancer diagnoses in Indonesia are expected to rise by 47% by 2020, with the death rate rising by 65.73%. According to the Indonesian Ministry of Health's cervical cancer clinical service guidelines, the chemotherapy used for cervical cancer is cisplatin, ifosfamide, 5-fluoro uracil, vinkristin, bleomycin, taxan, and carboplatin in combination form (Marth et al., 2017; Wu et al., 2021). Cisplatin is currently utilized in combination therapy due of its resistance. Chemotherapy, on the other hand, operates selectively in each stage of cancer growth and has a multidrug resistance mechanism. Therefore it has side effects and issues due to harm to normal cells (Paraswati & Subarnas, 2018).

The process of discovering cancer drug candidates continues. This is due to the resistance that occurs in cervical cancer therapy. Plant metabolite compounds are one source that can be used to explore new drug candidates. Cancer therapy is expected to achieve multi-targets as per the characteristics of cancer cells (Hanahan, 2022; He et al., 2020). Cancer therapy can use synthetic drugs or drugs made from natural ingredients.

Many natural medicines developed from natural ingredients are in the Zingiber family. *Zingiber striolatum* (Tian et al., 2020), *Zingiber griffithii* (Lutfia et al., 2021), *Zingiber zerumbet* (Diastuti et al., 2022), serta *Zingiber officinale* (Liao et al., 2020). *Zingiber officinale* (red ginger rhizome) has a better effect because it has the anti-emetic effect that is needed when used with cancer drugs. Red ginger rhizome has anticancer activity on HuH-7 and HeLa cells by inhibiting growth factors (González-Osuna et al., 2023). In addition, Jane red increases cytotoxic activity by increasing P21, CDK2, and CDK4, which inhibit cell proliferation (Mao et al., 2019). Research that has been carried out shows that extracts and essential oils are able to inhibit the growth of cervical cancer cells both in vitro and in vivo. The active compounds that have been isolated are 6-shogaol and 10-gingerol, with IC₅₀ values of 29.19 µM each and 25.68–37.52 µM (Zhang et al., 2021).

Anticancer development is carried out using in vitro, in vivo, and in silico methods. The *in silico* approach to exploring the mechanisms of anticancer drugs is very developed because it relates to the complex mechanisms of cancer and anticancers. However, this approach can be carried out when the compounds in the plant and the cancer therapy targets being studied are clearly defined (Shaker et al., 2021).

Cervical cancer therapy targets involve 15 pathways, namely ERK/MAPK, PI3K/Akt/mTOR, EGFR/VEGFR, apoptosis, Wnt/β-catenin, EMT, JAK/STAT, molecular YY-1, AP-1, NF-kB, CXXL12/CXCR4, Notch, Hippo, SOX, and Hedgehog (Bahrami et al., 2017; Bonab et al., 2021; Ciccamese et al., 2019; De Melo et al., 2017; Gutiérrez-Hoya & Soto-Cruz, 2020; Liu & Wang, 2019; Paskeh et al., 2021; Qureshi et al., 2015; Rodrigues et al., 2019; Scarth et al., 2021; Shi et al., 2019; Tilborghs et al., 2017; Yang et al., 2018). The 6-shogaol compound has been proven to be able to induce cell cycle arrest in the G2/M phase, activate apoptosis via the mitochondrial pathway, induce autophagy, suppress cell migration, and suppress the PI3K/Akt/mTOR pathway. The 10-gingerol compound has been proven to be able to induce cell cycle arrest in the G0/G1 phase, activate apoptosis through apoptosis indicators (Caspase family) and the mitochondrial pathway, suppress the PI3K/AKT pathway, activate AMPK, and suppress mTOR. The 6-gingerol compound induces cell cycle arrest in the G0/G1 phase, induces apoptosis through increasing the Bax/Bcl-2 ratio, releases cytochrome c, induces apoptosis through the AMPK activation cascade pathway, and suppresses PI3K/AKT and mTOR. Ginger extract and essential oil fractions have also been shown to stop cell growth by increasing prostaglandin production and inducing apoptosis (Ansari et al., 2016; Liu et al., 2012; Pei et al., 2021; Zhang et al., 2017b; Zhang et al., 2022; Zivarpour et al., 2021).

However, no research has been carried out regarding red ginger ethanol extract in HeLa cells with an anti-proliferation mechanism through inhibition of JAK2/STAT3 and hedgehog. The JAK2/STAT3 and hedgehog pathways are two pathways that play a role in the growth process of cervical cancer cells. Inhibition of these two pathways can cause cancer cells not to grow and undergo apoptosis.

Based on the results of GC-MS analysis of 75% ethanol extract of red ginger rhizomes, there are 25 compounds that have the potential to be candidates for cervical cancer drugs. This study aims to determine the cytotoxic effect of an ethanol extract of red ginger rhizome and screen the active compounds that have a cytotoxic effect on HeLa cells through their ability to be antiproliferative cells via the JAK2/STAT3 and hedgehog pathways using a molecular docking approach.

MATERIALS AND METHOD

Materials

The red ginger rhizomes used were obtained from UPTD Jamu Health Tourism, Tegal District Health Service. It has been determined by the Batu Herbal Materia Medica Laboratory UPT, East Java Provincial Health Service, with number 067/1410/102.20/2023.

6-Shogaol/6-S, 10-Gingerol/10-G (MarkHerb), cisplatin (Dankos), The 3D form compounds resulting from GC-MS analysis of 75% ethanol extract of red ginger rhizomes, Ethanol 96% (technical, Bratachem), aquadest (Bratachem) NaOH (Merck), methanol p.a. (Merck), HeLa cell culture collection from the UGM Faculty of Medicine Parasitology Laboratory, aquabidest, sodium bicarbonate (Sigma), hepes (Sigma), RPMI media, fetal bovine serum (FBS) 10% v/v (Gibco), penicillin-streptomycin 1% v/v (Gibco), fungion 0.5% (Gibco), phosphate buffer saline (PBS) 20% (Sigma), dimethyl sulfoxo (DMSO), MTT Reagent (3-(4,5-Dimethylthiazol-2-yl)-2,5-diphenyltetrazolium bromide) 5 mg in 1 mL PBS (Sigma), stopper, sodiun dodecyl (SDS) 10% in HCL 0.01 N (Merck), 96-well plate, trytan blue stain 0.25% (Gibco). Molecular docking was carried out using PyRx 0.8 Autodock 4.0 software; receptor and native ligand preparation was done using visualization of docking results using Biovia Discovery Studio. Receptors JAK2 (PDB code: 6vgl), STAT3 (PDB code: 6nuq), and SMO (PDB code: 517i) were obtained from the Research Collaboratory for Structural Bioinformatics (RCSB) Protein Data Bank website (www.rcsb.org).

Instrumentation

Rotary evaporator (Heidolph), freeze dryer (Ilshinbiobase), desktop-AFDBVC8, processor Intel@CoreTMi5-4440 CPU @3.10GHz, RAM 8GB; CO₂ incubator (New Brunswick, Galaxy 170R) centrifuge (Hermle Siemensstr-25 D-78564), laminar air flow (LAF) cabinet (Mascotte LH-S, micropipette (Soccorex), autoclave, hemocytometer, ELISA reader (Robonik), and inverted microscope (Olympus CKX41-2).

Methods

Extraction

Reg ginger rhizome powder was extracted using the remaceration method using a 75% ethanol solvent. Concentrate the extract using a rotary evaporator at a pressure of 100–105 mbar, 60 rpm, and a water bath temperature of 50°C until a volume of 100 mL is obtained. Next, concentration was carried out using freeze drying at a temperature of -56°C and a pressure of 0.05 mTorr for 48 hours. The extract was stored at -20°C.

MTT assay cytotoxicity

The MTT assay was used in cytotoxicity testing. HeLa cell cultures were plated at a density of 5×10^4 cells/well in 96-well plates, and they were incubated for 24 hours at 37°C in a CO₂ incubator. After adding the test sample solution, the cell culture was placed in a CO₂ incubator and left for a full day. After adding 0.5 mg/mL MTT solution, the mixture was incubated for 2–4 hours at 37°C in a CO₂ incubator, or until formazan crystals appeared. After adding a 10% SDS/0.01 N HCl solution, the plates were covered with aluminium foil, left overnight at room temperature, and kept in a dark location.

Molecular docking analysis

Receptor preparation

The JAK2, STAT3, and SMO receptors were obtained from the Protein Data Bank with the codes 6vgl, 6nuq, and 517i, respectively, in 3D form. Preparation was carried out by separating the receptor from the native ligand using the Biovia Discovery Studio application.

Method validation

Validation was performed by redocking the natural ligand molecule on the receptor. Ruxolitinib is the natural ligand for the 6vgl, 6nuq, and 517i receptors, [(2- {[[(5S,8S,10aR)3-acetyl-8- ((2S)5-amino-1-[(Aminomethyl) phenyl] carbamoyl-1,5-dioxopentan-2-yl) [1,2-a] 6-oxodecahydropyrrolo [1,5]carbamoyl]diazocin-5-yl]-1H-indol-5-yl) (difluoro) methyl], vismodegib, and phosphonic acid/KQV. GA run = 100, maximum number of energy assessments = 2,500,000, population size = 150, and maximum generation = 27,000 were the parameters used for the docking technique. When the root mean square deviation (RMSD) value was less than two standard deviations, it was acceptable to conduct and declare receptor research as valid.

Preparation of test compounds

Redocking the receptor's native ligand molecule serves as validation. The natural ligand for the 6vgl, 6nuq, and 517i receptors is ruxolitinib. [(2- {[[(5S,8S,10aR)3-acetyl-8- ((2S)5-amino-1-[phenyl (aminomethyl)] [1,2-a] carbamoyl-1,5-dioxopentan-2-yl [1,5] 6-oxodecahydropyrrolo [carbamoyl]vismodegib, phosphonic acid/KQV, and diazocin-5-yl-1H-indol-5-yl)(difluoro)methyl. The parameters for the docking technique were GA run = 100, maximum number of energy assessments = 2,500,000, population size = 150, and maximum generation = 27,000. Receptor study can be conducted and deemed genuine when the root mean square deviation (RMSD) value was less than two standard deviations.

Molecular docking simulation process

The PyRx 0.8 Autodock 4.0 software was used to run the simulation. With the receptor coordinates 6vgl: 8.672087; -27.316174; 53.313304; 6nuq receptor: 13.126458; 55.609983; 0.109915; 517i receptor: 5.490333; 56.168667; -39000333, distance 0.3750 Å, the grid box's dimensions were adjusted to x: 65, y: 65, and z: 65. Additionally, a genetic algorithm with a total GA run of 100, a maximum of 2,500,000 energy assessments, a population size of 150, and a maximum generation of 27,000 was employed.

Molecular docking simulation

The ligands were then saved in PDBQT format, and the molecular docking simulation to screen the potential ligands was carried out using validated parameters from control docking. The visualization of docking simulations was performed using Biovia Discovery Studio Visualizer, and the results were sorted based on the free energy of binding on the most populated cluster and their intermolecular interactions with receptors.

Data Analysis

Molecular docking results were analyzed using Biovia Discovery Studio Visualizer. Interactions with amino acid residues, inhibition constants, and binding free energies were the parameters considered. Determining the best ligand conformation resulting from molecular docking was based on these parameters.

RESULT AND DISCUSSION

Extraction

The extract produced in this research meets the provisions stated in the Indonesian Herbal Pharmacopoeia (FHI) edition II ([Kementerian Kesehatan RI, 2017](#)). The description data contained in

the Indonesian Herbal Pharmacopoeia II edition states that red ginger rhizome extract has the characteristics of a thick extract, brownish yellow, a distinctive odor with a spicy taste, and an extract yield of 18%, not less than 17.0% w/w.

Table 1. Simplicia and 75 % ethanolic extract of characterization of the red ginger rhizomes

Samples	Organoleptic		
	Colour	Odor	Taste
Simplicia	Brown	Strong aromatic	Spicy
75 % of Ethanolic extract	Yellowish brown	Strong aromatic	Spicy

MTT assay cytotoxicity

The inhibitory ability of a 75% ethanol extract from red ginger rhizomes was lower than cisplatin, 6-shogaol, and 10-gingerol ($p < 0.05$). The results of the cytotoxicity test are presented in Table 2. The results of this study confirm the results of previous research that the compounds 6-shogaol, 10-gingerol, and components of the terpenoid group contained in red ginger rhizomes have the ability to inhibit the growth of HeLa cancer cell cultures (Lee, 2016; Okumura et al., 2012; Pei et al., 2021; Zhang et al., 2017a).

Table 2. Cytotoxicity assay by MTT method

Samples	IC ₅₀ in HeLa cell lines			$\bar{x} \pm SD$
	($\mu\text{g/mL}$)			
	1	2	3	
75 % Ethanolic extract	108.03	97.09	107.55	104.22 \pm 6.18
6-Shogaol	59.82	42.78	39.33	47.31 \pm 10.97 ^(*)
10-Gingerol	50.54	42.56	54.38	49.16 \pm 6.03 ^(*)
Cisplatin	40.67	39.11	46.59	38.61 \pm 3.66 ^(*)

*significant differences $p < 0,05$

Molecular docking analysis

The method validation process is carried out by redocking the native ligand with the receptor. The results of the validation process show RMSD $< 2,000$ Å. These results indicate that the docking process is valid (Suhandi et al., 2021). The results of the molecular docking validation process are presented in Table 3 and Figure 1.

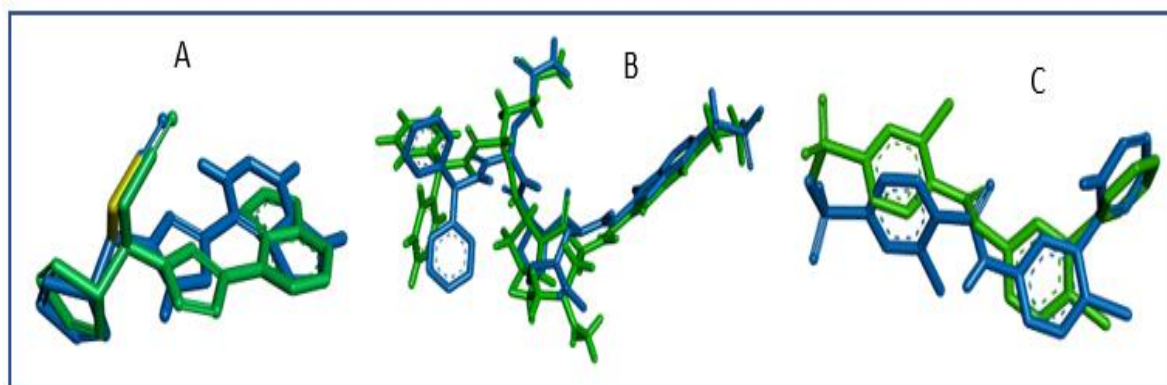


Figure 1. Overlay of native ligand pre-docking (blue) and re-docking (green), A. Ruxolitinib, B. KQV, C. vismodegib

Table 3. Validation of molecular docking method

Receptor	Native Ligand	RMSD (Root-Mean-Square Deviation)	Binding energy (kcal/mol)	Inhibition constant/IC (mikroMolar/ uM)
JAK2 (PDB code: 6vgl)	Ruxolitinib	1.384 A	-8.40	0.69184
STAT3 (PDB code: 6nuq)	[(2-{{[(5S,8S,10aR)]3-acetyl-8-((2S)5-amino-1-[(Aminomethyl)phenyl]carbamoyl-1,5-dioxopentan-2-yl)[1,2-a] 6-oxodecahydropyrrolo[1,5]carbamoyl]diazocin-5-yl}Phosphoric acid/KQV vismodegib (1H-indol-5-yl)(difluoro)methyl	1.687 A	-12.10	0.00136
SMO (PDB code: 5I7i)		1.674 A	-10.47	0.02110

The JAK2 receptor with the PDB code 6vgl is a crystal of the protein-ligand complex of JAK2 and ruxolitinib obtained from the purification of Expi293 mammalian cells. The ruxolitinib compound interacts with the JAK2 receptor via hydrogen bonds at amino acid residues Glu 930 and Leu 932. Hydrophobic interactions via van der Waals bonds also occur at amino acid residues Leu 855 and Gly 856. The inhibitory ability of ruxolitinib on the growth of myeloproliferative neoplasms, namely UKE-1 cells, has an IC₅₀ of 0.1–6.3 μ M, while testing using a radiometric assay shows an IC₅₀ value of 0.26–11.0 nM (Davis et al., 2021).

The crystal of the STAT3 receptor, which has the PDB code 6nuq, is a protein-ligand complex consisting of STAT3 and the substance [(2-{{[(5S,8S,10aR) 3-acetyl-8-((2S) 5-amino -1-[Amino [diphenylmethyl]] Pentan-2-yl carbamoyl-1,5-iodo Diazocin-5-yl]carbamoyl} 6,2-dioxo octahydro pyrrolo [1,2-a] [1,5] diazocin phosphonic acid/KQV (1H-indol-5-yl) (difluoro) methyl], which was produced by incubating STAT3 with KQV compound for three hours at 4°C. Hydrogen bond interactions of the KQV compound with the STAT3 receptor at amino acid residues Arg609, Ser611, Ser613, Glu612, Pro639, Ser636, Gln644, Tyr640, Lys658, Tyr657. Hydrophobic interactions at amino acid residues Leu 666, met 660, Ile 659. The ability of the KQV compound to inhibit MOLM16 leukemia cancer cells has an IC₅₀ value of 3 μ M (Davis et al., 2021).

The SMO receptor with the PDB code 5I7i is a protein-ligand complex crystal of smo and vismodegib. The mechanism of action of vismodegib is to compete for cholesterol receptors. Cholesterol in the hedgehog pathway supports the shh ligand to bind PTCH1 and supports smo to bind SUFU, causing the transcription factor gli1 to accumulate in the cell nucleus. Gli1 accumulation was shown to activate proliferation factors such as cyclin-D1 and MYC. Vismodegib hydrogen bond interactions occur at amino acid residues Asp384, Gln 477, and Arg400. Hydrophobic interactions occur at amino acid residues Phe484 and Asp473 (Byrne et al., 2016; Rimkus et al., 2016).

The predicted results of the activity of metabolite compounds in the JAK2/STAT3 and hedgehog pathways tested in silico using Autodock 4.0 software are presented in Table 4. The results show that in the JAK2 receptor, there are 2 potential compounds, namely alpha-cedrol and beta-eudesmol, with binding energy values and inhibition constants (K_i) respectively of -7.47 kcal/mol, -7.48 kcal/mol, and 3.33 μ M and 3.27 μ M. The ruxolitinib compound, which is a native ligand for the JAK2 receptor (PDB code: 6vgl), has binding energy and inhibition constant (K_i) values of -8.42 kcal/mol and 0.678 μ M.

Table 5 shows that the receptor interaction with the beta-eudesmol compound is similar to that of the ruxolitinib compound compared to the alpha-cedrol compound. The beta-eudesmol compound has the same hydrogen bonds as the ruxolitinib compound, namely to the amino acid glycine and alkyl bonds to the amino acid leucine. The alpha-cedrol compound has a lower bond energy value compared to beta-eudesmol because the alpha-cedrol compound has two hydrogen bonds, while the beta-eudesmol compound has only one hydrogen bond. The number of hydrogen bonds is an important predictor of the bioavailability of a compound (Agoni et al., 2020; Praceka et al., 2022).

Table 4. Prediction of binding activity and constant of inhibition active metabolite of red ginger rhizome by JAK2/STAT3 and hedgehog pathway

Receptor	Compounds	Binding energy (kcal/mol)	Inhibition constant/IC (mikroMolar/uM)
JAK2 (PDB code: 6vgl)	6-Methyl-5-Hepten-2-One	-4,43	568.27
	Octanal	-3,52	2640
	Borneol L	-5,6	78.51
	Decanal	-3,94	1290
	beta.-Citronellol	-4,55	463.94
	Geraniol	-4,74	335.45
	2-Octenal, 2-butyl-	-4,91	250.60
	trans-.beta.-Farnesene	-5,51	90.85
	Benzene, 1-(1,5-dimethyl-4-hexenyl)-4-methyl-	-6,19	29.21
	Zingiberene	-6,43	19.19
	Farnesol	-5,76	60.00
	beta.-Sesquiphellandrene	-6,57	15.24
	Trans-.Gamma.-Bisabolene	-6,58	15.12
	Cubenol	-7,04	6.88
	alpha.-Cedrol	-7,47*	3.33
	beta.-Bisabolene	-6,4	20.23
	sesquisabinene hydrate	-6,32	23.34
	Trans(.Beta.)-Caryophyllene	-6,77	10.90
	beta.-Eudesmol	-7,48*	3.27
	1H-Cycloprop[e]azulen-4-ol, decahydro-1,1,4,7-tetramethyl-, [1ar (1a.alpha.,4.alpha.,4a.beta.,7.alpha.,7a.beta.,7b.alpha.)]-(C	-7	7.46
	cis-Farnesol	-5,82	54.32
	6,10-Dodecadien-1-yn-3-ol, 3,7,11-trimethyl	-6,12	32.87
	Campherone	-6,14	31.36
	Pentadecanoic acid, 14-methyl-, methyl ester	-4,79	310.72
	9-Octadecenoic acid (Z)-, methyl ester	-5,14	171.07
	Ruxolitinib (Native Ligand 6vgl)	-8,42	0.678

Receptor	Compounds	Binding energy (kcal/mol)	Inhibition constant/IC (mikroMolar/uM)
STAT3 (kode PDB: 6nuq)	6-Methyl-5-Hepten-2-One	-3,66	2090
	Octanal	-3,03	5990
	Borneol L	-4,53	477.17
	Decanal	-3,26	4070
	beta.-Citronellol	-3,95	1270
	Geraniol	-3,83	1550
	2-Octenal, 2-butyl-	-3,65	2110
	trans.-beta.-Farnesene	-4,27	737.16
	Benzene, 1-(1,5-dimethyl-4-hexenyl)-4-methyl-	-4,73	338.66
	Zingiberene	-5,05	200.29
	Farnesol	-4,52	488.49
	beta.-Sesquiphellandrene	-5	215.53
	Trans-.Gamma.-Bisabolene	-4,97	226.82
	Cubenol	-5,54	86.38
	alpha.-Cedrol	-5,33	124.29
	beta.-Bisabolene	-5	217.50
	sesquisabinene hydrate	-5,28	135.37
	Trans(.Beta.)-Caryophyllene	-5	216.12
	beta.-Eudesmol	-6,05*	36.48
	1H-Cycloprop[e]azulen-4-ol, decahydro-1,1,4,7-tetramethyl-, [1ar (1a.alpha.,4.alpha.,4a.beta.,7.alpha.,7a.beta.,7b.alpha.)]- (C		
	cis-Farnesol	-4,5	503.03
	6,10-Dodecadien-1-yn-3-ol, 3,7,11-trimethyl	-4,98	223.89
	Campherenone	-5,33	123.84
	Pentadecanoic acid, 14-methyl-, methyl ester	-3,67	2030
	9-Octadecenoic acid (Z)-, methyl ester	-3,46	2900
	[(2-{{(5S,8S,10aR)-3-acetyl-8-{{(2S)-5-amino-1-[[diphenylmethyl]amino]-1,5-dioxopentan-2-yl}carbamoyl)-6-oxodecahydropyrrolo[1,2-a][1,5]diazocin-5-yl}carbamoyl}-1H-indol-5-yl)(difluoro)methyl]phosphonic acid/KQV (Native Ligand 6nuq)	-12,1	0.00136

Receptor	Compounds	Binding energy (kcal/mol)	Inhibition constant/IC (mikroMolar/ uM)
SMO (PDB code: 517i)	6-Methyl-5-Hepten-2-One	-4,2	841.10
	Octanal	-3,72	1870
	Borneol L	-5,64	74.04
	Decanal	-4,03	1120
	beta.-Citronellol	-4,87	268.73
	Geraniol	-4,94	237.50
	2-Octenal, 2-butyl-	-5,19	156.61
	trans-.beta.-Farnesene	-6,08	34.94
	Benzene, 1-(1,5-dimethyl-4-hexenyl)-4-methyl-	-6,41	20.14
	Zingiberene	-6,93	8.29
	Farnesol	-6,31	23.76
	beta.-Sesquiphellandrene	-7,03	7.03
	Trans-.Gamma.-Bisabolene	-6,71	12.09
	Cubenol	-7,17	5.56
	alpha.-Cedrol	-7,3	4.44
	beta.-Bisabolene	-6,83	9.92
	sesquisabinene hydrate	-6,76	11.11
	Trans(.Beta.)-Caryophyllene	-7,21	5.16
	beta.-Eudesmol	-7,57*	2.81
	1H-Cycloprop[e]azulen-4-ol, decahydro-1,1,4,7-tetramethyl-, [1ar (1a.alpha.,4.alpha.,4a.beta.,7.alpha.,7a.beta.,7b.alpha.)]-(C		
	cis-Farnesol	-6,48	17.75
	6,10-Dodecadien-1-yn-3-ol, 3,7,11-trimethyl	-6,7	12.36
	Campherenone	-7,05	6.80
	Pentadecanoic acid, 14-methyl-, methyl ester	-5,41	107.71
	9-Octadecenoic acid (Z)-, methyl ester	-5,88	48.60
	vismodegib (Native Ligand 517d)	-10,43	0.02251

* Lowest binding energy

The 75% ethanol extract compound of red ginger rhizomes that has inhibitory potential for STAT3 receptors is the compound beta-Eudesmol, with binding energy and inhibition constant (K_i) values of -6.05 kcal/mol and 36.48 uM, respectively. However, the inhibitory ability of this compound is lower than 282 that of the native ligand KQV at the state 3 receptor (PDB code: 6nuq). The binding energy and inhibition constant (K_i) values for the KQV compound are -12.1 kcal/mol and 0.00136 uM. The similarity in the interaction of the beta-Eudesmol compound with the KQV compound in the alkyl bond at the amino acid residue Lys 658.

Prediction of inhibition of the hedgehog pathway with the SMO receptor (PDB code: 517i) shows that the compound with a binding energy value of -7.57 kcal/mol and a K_i value of 2.81 uM is a beta-Eudesmol compound. The native ligand for the SMO receptor (PDB code: 517i), namely the compound

vismodegib, provides a binding energy value of -10.43 kcal/mol and a K_i value of 0.02251 μM . Similarity in the interaction of the beta-Eudesmol compound with the KQV compound in the alkyl bond in the amino acid residue Pro513. It is necessary to carry out combination docking with other software, for example PLANTS, because the software here is not yet available for combination docking.

MS chromatograms of compounds and the chemical structures of compounds that have anti-proliferative potential via the JAK2/STAT3 and hedgehog pathways *in silico* are presented in Figure 2. According to the constituent functional groups, these active compounds belong to the sesquiterpene group of compounds. Receptor interactions with compounds or ligands *in silico* testing are presented in Table 5 and Figures 3-5.

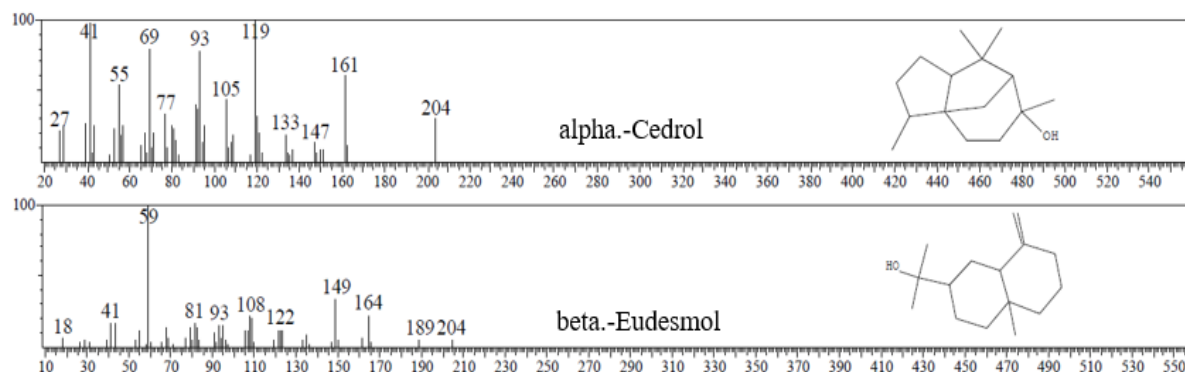


Figure 2. The MS and chemical structure of active metabolite in JAK2/STAT3 and hedgehog pathway

Table 5. The type of interaction between *native ligand/active compound* with proteins

Receptor	Compounds	Amino acid residues	
		Hydrogen Bonding	Other Binding
JAK2 (kode PDB: 6vgl)	Ruxolitinib	Gly 993; Glu 930	Leu 855; Ala 880; Leu 983; Val 863; Asp 994
	alpha.-Cedrol	Lys 882; Asp 994	His 891; Phe 860; Gly 996
	beta.-Eudesmol	Gly 858	Leu 884; Phe 860; His 891
STAT3 (kode PDB: 6nuq)	[(2-{{(5S,8S,10aR)-3-acetyl-8-((2S)-5-amino-1-[(diphenylmethyl)amino]-1,5-dioxopentan-2-yl)carbamoyl)-6-oxodecahydropyrrolo[1,2-a][1,5]diazocin-5-yl)carbamoyl]-1H-indol-5-yl)(difluoro)methyl]phosphonic acid (KQV)	Ser 636; Glu 638; Gln 644; Pro 639; Ser 613; Glu 612	Lys 658; Ile 659; Val 637; Arg 609; Ser 611
SMO (kode PDB: 517i)	beta.-Eudesmol	Ile 653; Tyr 640	Lys 658
	vismodegib	Tyr 394, Asp 384	Pro 513, Asn 219, Met 230, His 470, Leu 522, Trp 281, Val 386, Glu 518
	beta.-Eudesmol	Glu 481, Lys 395	Pro 513

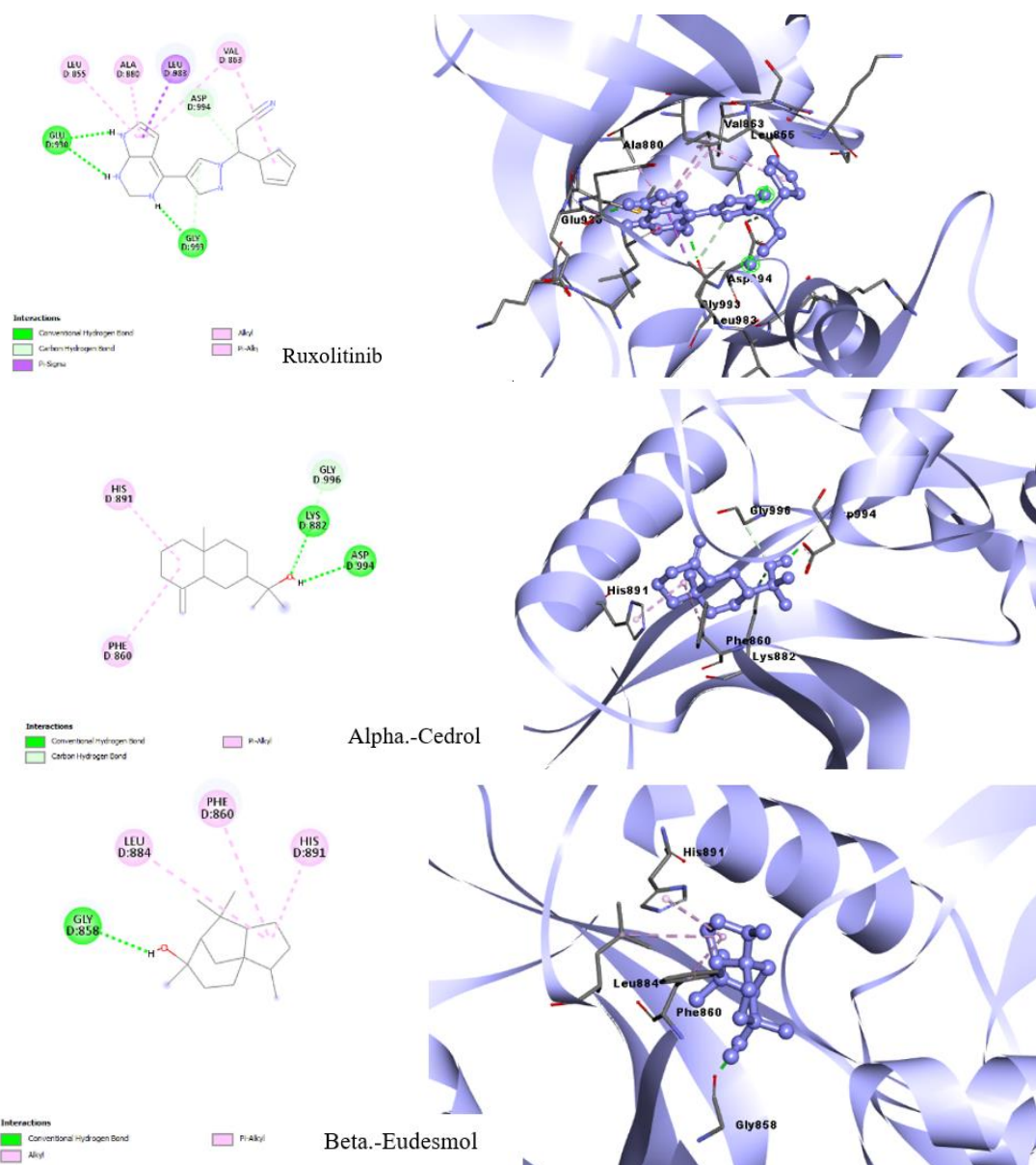


Figure 3. The 2D and 3D visualization of the interaction of native ligand (a) and active compounds (b and c) with JAK2 receptor (PDB code: 6vgl)

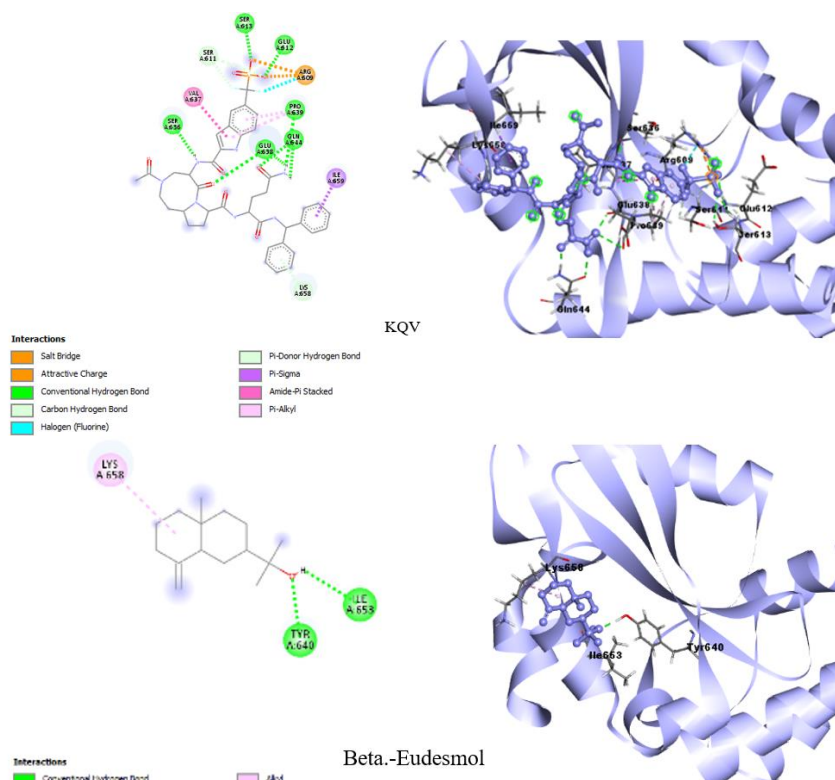


Figure 4. The 2D and 3D visualization of the interaction of native ligand (a) and active compounds (b and c) with STAT3 receptor (PDB code: 6nuq)

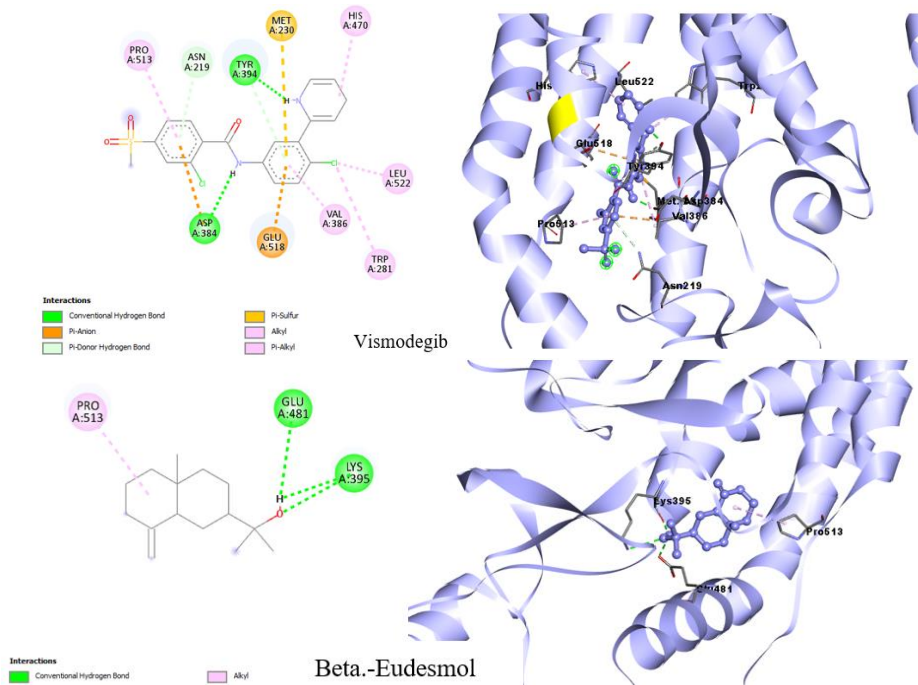


Figure 5. The 2D and 3D visualization of interaction of native ligand (a) and active compounds (b and c) with 517i receptor (PDB code: 517i)

CONCLUSION

The 75% ethanol extract of red ginger rhizomes has antiproliferative activity against the growth of HeLa cancer cells with an IC_{50} value of $104.22 \pm 6.18 \mu\text{g/mL}$. The active compounds predicted to be able to inhibit cell proliferation via the JAK2/STAT3 and hedgehog pathways using an *in silico* approach are the compounds alpha-cedrol and beta-beta-eudesmol.

ACKNOWLEDGEMENT

The Ministry of Education and Culture, Innovative and Research Council, Indonesia provided financial assistance for this work through Postgraduate Research Grant (No. 0536/E5/PG.02.00/2023).

REFERENCES

- Agoni, C., Olotu, F. A., Ramharack, P., & Soliman, M. E. (2020). *Druggability and drug-likeness concepts in drug design: are biomodelling and predictive tools having their say?* <https://doi.org/10.1007/s00894-020-04385-6>
- Ansari, J. A., Ahmad, M. K., Khan, A. R., Fatima, N., Khan, H. J., Rastogi, N., Mishra, D. P., & Mahdi, A. A. (2016). Anticancer and antioxidant activity of *Zingiber officinale roscoe* rhizome. *Indian Journal of Experimental Biology*, 54(11), 767–773. <https://doi.org/10.9734/BJPR/2016/26198>
- Bahrami, A., Hasanzadeh, M., ShahidSales, S., Yousefi, Z., Kadkhodayan, S., Farazestanian, M., Joudi Mashhad, M., Gharib, M., Mahdi Hassanian, S., & Avan, A. (2017). Clinical significance and prognosis value of wnt signaling pathway in cervical cancer. *Journal of Cellular Biochemistry*, 118(10), 3028–3033. <https://doi.org/10.1002/jcb.25992>
- Bonab, F. R., Baghbanzadeh, A., Ghaseminia, M., Bolandi, N., Mokhtarzadeh, A., Amini, M., Dadashzadeh, K., Hajiasgharzadeh, K., Baradaran, B., & Baghi, H. B. (2021). Molecular pathways in the development of hpv-induced cervical cancer. *EXCLI Journal*, 20, 320–337. <https://doi.org/10.17179/excli2021-3365>
- Byrne, E. F. X., Sircar, R., Miller, P. S., Hedger, G., Luchetti, G., Nachtergaele, S., Tully, M. D., Mark, S. P., Mydock-mcgrane, L., Covey, D. F., & Robert, P. (2016). Structural basis of Smoothed regulation by its extracellular domains. *Nature*, 1–21. <https://doi.org/10.1038/nature18934>
- Cibula, D., Poetter, R., & Raspollini, M. R. 2018. Cervical cancer guidelines. In *European Society of Gynaecological Oncology*. [https://doi.org/10.1016/S0140-6736\(86\)92243-9](https://doi.org/10.1016/S0140-6736(86)92243-9)
- Ciccarese, F., Zulato, E., & Indraccolo, S. (2019). LKB1/AMPK Pathway and Drug Response in Cancer: A Therapeutic Perspective. *Oxidative Medicine and Cellular Longevity*, 2019. <https://doi.org/10.1155/2019/8730816>
- Davis, R. R., Li, B., Yun, S. Y., Chan, A., Nareddy, P., Gunawan, S., Ayaz, M., Lawrence, H. R., Reuther, G. W., Lawrence, N. J., & Schönbrunn, E. (2021). Structural Insights into JAK2 Inhibition by Ruxolitinib, Fedratinib, and Derivatives Thereof. *Journal of Medicinal Chemistry*, 64(4), 2228–2241. <https://doi.org/10.1021/acs.jmedchem.0c01952>
- De Melo, A. C., Paulino, E., & Garces, Á. H. I. (2017). A Review of mTOR Pathway Inhibitors in Gynecologic Cancer. *Oxidative Medicine and Cellular Longevity*, 2017. <https://doi.org/10.1155/2017/4809751>
- Diastuti, H., Asnani, A., Delsy, E. V. Y., Pamukasari, R., & Indriani, S. (2022). Toxicity and Antimicrobial Activity of Zerumbon from *Zingiber zerumbet* Rhizome. *Molekul*, 17(3), 328. <https://doi.org/10.20884/1.jm.2022.17.3.5808>
- González-Osuna, J. O., Barbabosa-Pliego, A., Tenorio-Borroto, E., Chávez-Salinas, S., Alonso-Fresan, M. U., Contreras-Ortiz, J. M. E., Vázquez-Chagoyan, J. C., López-Valdez, L. G., Reyes, C., Herrera-Cabrera, B. E., Zaragoza-Martínez, F., Lucho-Constantino, G. G., & Barrales-Cureño, H. J. (2023). Evaluation of extracts from *Curcuma longa* and *Zingiber officinale* as growth inhibitors of HeLa and HuH-7 Cell Lines. In *Plant-Derived Anticancer Drugs in the OMICS Era* (pp. 1–24). Apple Academic Press. <https://doi.org/10.1201/9781003377412-1>

- Gutiérrez-Hoya, A., & Soto-Cruz, I. (2020). Role of the JAK/STAT Pathway in Cervical Cancer: Its Relationship with HPV E6/E7 Oncoproteins. *Cells*, 9(10), 1–22. <https://doi.org/10.3390/cells9102297>
- Hanahan, D. (2022). Hallmarks of cancer: new dimensions. *Cancer Discovery*, 12(1), 31–46. <https://doi.org/10.1158/2159-8290.CD-21-1059>
- He, B., Zhao, Z., Cai, Q., Zhang, Y., Zhang, P., Shi, S., Xie, H., Peng, X., Yin, W., Tao, Y., & Wang, X. (2020). Mirna-based biomarkers, therapies, and resistance in cancer. *International Journal of Biological Sciences*, 16(14), 2628–2647. <https://doi.org/10.7150/ijbs.47203>
- Kementerian Kesehatan RI. (2017). *Farmakope Herbal Indonesia*. Kementerian Kesehatan Republik Indonesia.
- Lee, Y. (2016). Cytotoxicity evaluation of essential oil and its component from *Zingiber officinale* Roscoe. *Toxicological Research*, 32(3), 225–230. <https://doi.org/10.5487/TR.2016.32.3.225>
- Liao, D., Cheng, C., Liu, J., Zhao, L., Huang, D.-C., & Chen, G. (2020). Characterization and antitumor activities of polysaccharides obtained from ginger (*Zingiber officinale*) by different extraction methods. *International Journal of Biological Macromolecules*, 152, 894–903. <https://doi.org/10.1016/j.ijbiomac.2020.02.325>
- Liu, C., & Wang, R. (2019). The roles of hedgehog signaling pathway in radioresistance of cervical cancer. *Dose-Response*, 17(4), 1–5. <https://doi.org/10.1177/1559325819885293>
- Liu, Y., Whelan, R. J., Pattnaik, B. R., Ludwig, K., Subudhi, E., Rowland, H., Claussen, N., Zucker, N., Uppal, S., Kushner, D. M., Felder, M., Patankar, M. S., & Kapur, A. (2012). Terpenoids from *Zingiber officinale* (Ginger) induce apoptosis in endometrial cancer cells through the activation of p53. *PLoS ONE*, 7(12). <https://doi.org/10.1371/journal.pone.0053178>
- Lutfia, A., Munir, E., Yurnaliza, Y., & Basyuni, M. (2021). Chemical analysis and anticancer activity of sesterterpenoid from an endophytic fungus *Hypomontagnella monticulosa* Zg15SU and its host *Zingiber griffithii* Baker. *Heliyon*, 7(2), e06292. <https://doi.org/10.1016/j.heliyon.2021.e06292>
- Mao, Q.-Q., Xu, X.-Y., Cao, S.-Y., Gan, R.-Y., Corke, H., & Li, H.-B. (2019). Bioactive compounds and bioactivities of ginger (*Zingiber officinale* Roscoe). *Foods*, 8(6), 185.
- Marth, C., Landoni, F., Mahner, S., McCormack, M., Gonzalez-Martin, A., & Colombo, N. (2017). Cervical cancer: ESMO Clinical Practice Guidelines for diagnosis, treatment and follow-up. *Annals of Oncology*, 28(Supplement 4), iv72–iv83. <https://doi.org/10.1093/annonc/mdx220>
- Okumura, N., Yoshida, H., Nishimura, Y., Kitagishi, Y., & Matsuda, S. (2012). Terpinolene, a component of herbal sage, downregulates AKT1 expression in K562 cells. *Oncology Letters*, 3(2), 321–324. <https://doi.org/10.3892/ol.2011.491>
- Paraswati, & Subarnas, A. (2018). Review: Aktivitas Tanaman Sablo (*Acalypha wilkesiana* Müll.Arg.) Sebagai Antikanker Serviks. *Farmaka*, 16(2), 33–41.
- Paskeh, M. D. A., Mirzaei, S., Gholami, M. H., Zarrabi, A., Zabolian, A., Hashemi, M., Hushmandi, K., Ashrafizadeh, M., Aref, A. R., & Samarghandian, S. (2021). Cervical cancer progression is regulated by SOX transcription factors: Revealing signaling networks and therapeutic strategies. *Biomedicine and Pharmacotherapy*, 144, 112335. <https://doi.org/10.1016/j.biopha.2021.112335>
- Pei, X.-D., He, Z.-L., Yao, H.-L., Xiao, J.-S., Li, L., Gu, J.-Z., Shi, P.-Z., Wang, J.-H., & Jiang, L.-H. (2021). 6-Shogaol from ginger shows anti-tumor effect in cervical carcinoma via PI3K/Akt/mTOR pathway. *European Journal of Nutrition*, 60(5), 2781–2793. <https://doi.org/10.1007/s00394-020-02440-9>
- Praceka, M. S., Yunita, E. N., Semesta, C. D., Putri, R. N., & Tenggara, A. (2022). *Molecular Docking and Toxicity from Temulawak Rhizome (Curcuma xanthorrhiza Roxb .) against COX-2 Penambatan Molekul dan Toksisitas dari Rimpang Temulawak (Curcuma xanthorrhiza Roxb .) terhadap COX-2*. 1(1).
- Qureshi, R., Arora, H., & Rizvi, M. A. (2015). EMT in cervical cancer: Its role in tumour progression and response to therapy. *Cancer Letters*, 356(2), 321–331. <https://doi.org/10.1016/j.canlet.2014.09.021>

- Rimkus, T. K., Carpenter, R. L., Qasem, S., Chan, M., & Lo, H. (2016). *Targeting the Sonic Hedgehog Signaling Pathway: Review of Smoothed and GLI Inhibitors*. 1–23. <https://doi.org/10.3390/cancers8020022>
- Rodrigues, C., Joy, L. R., Sachithanandan, S. P., & Krishna, S. (2019). Notch signalling in cervical cancer. *Experimental Cell Research*, 385(2), 111682. <https://doi.org/10.1016/j.yexcr.2019.111682>
- Scarth, J. A., Patterson, M. R., Morgan, E. L., & Macdonald, A. (2021). The human papillomavirus oncoproteins: A review of the host pathways targeted on the road to transformation. *Journal of General Virology*, 102(3). <https://doi.org/10.1099/JGV.0.001540>
- Shaker, O., Ayseldeen, G., & Abdelhamid, A. (2021). The impact of single nucleotide polymorphism in the Long Non-coding MEG3 Gene on MicroRNA-182 and MicroRNA-29 Expression Levels in the Development of Breast Cancer in Egyptian Women. *Frontiers in Genetics*, 12. <https://doi.org/10.3389/fgene.2021.683809>
- Shi, X., Wang, J., Lei, Y., Cong, C., Tan, D., & Zhou, X. (2019). Research progress on the PI3K/AKT signaling pathway in gynecological cancer (Review). *Molecular Medicine Reports*, 19(6), 4529–4535. <https://doi.org/10.3892/mmr.2019.10121>
- Suhandi, C., Fadhilah, E., Silvia, N., & Atusholihah, A. (2021). *Molecular Docking Study of Mangosteen (Garcinia mangostana L.) Xanthone-Derived Isolates as Anti Androgen*. February, 11–20.
- Tian, M., Wu, X., Hong, Y., Wang, H., Deng, G., & Zhou, Y. (2020). Comparison of Chemical Composition and Bioactivities of Essential Oils from Fresh and Dry Rhizomes of Zingiber zerumbet (L.) Smith. *BioMed Research International*, 2020, 1–9. <https://doi.org/10.1155/2020/9641284>
- Tilborghs, S., Corthouts, J., Verhoeven, Y., Arias, D., Rolfo, C., Trinh, X. B., & van Dam, P. A. (2017). The role of Nuclear Factor-kappa B signaling in human cervical cancer. *Critical Reviews in Oncology/Hematology*, 120(November), 141–150. <https://doi.org/10.1016/j.critrevonc.2017.11.001>
- Wu, T. N., Chen, H. M., & Shyur, L. F. (2021). Current advancements of plant-derived agents for triple-negative breast cancer therapy through deregulating cancer cell functions and reprogramming tumor microenvironment. *International Journal of Molecular Sciences*, 22(24). <https://doi.org/10.3390/ijms222413571>
- Yang, M., Wang, M., Li, X., Xie, Y., Xia, X., Tian, J., Zhang, K., & Tang, A. (2018). Wnt signaling in cervical cancer? *Journal of Cancer*, 9(4), 659–668. <https://doi.org/10.7150/jca.22005>
- Zhang, F., Thakur, K., Hu, F., Zhang, J.-G., & Wei, Z.-J. (2017a). 10-Gingerol, a Phytochemical derivative from Tongling White Ginger, inhibits cervical cancer: insights into the molecular mechanism and inhibitory targets. *Journal of Agricultural and Food Chemistry*, 65(10), 2089–2099. <https://doi.org/10.1021/acs.jafc.7b00095>
- Zhang, F., Thakur, K., Hu, F., Zhang, J. G., & Wei, Z. J. (2017b). 10-Gingerol, a Phytochemical Derivative from Tongling White Ginger, inhibits cervical cancer: insights into the molecular mechanism and inhibitory targets. *Journal of Agricultural and Food Chemistry*, 65 (10). <https://doi.org/10.1021/acs.jafc.7b00095>
- Zhang, M., Zhao, R., Wang, D., Wang, L., Zhang, Q., Wei, S., Lu, F., Peng, W., & Wu, C. (2021). Ginger (Zingiber officinale Rosc.) and its bioactive components are potential resources for health beneficial agents. *Phytotherapy Research*, 35(2), 711–742. <https://doi.org/10.1002/ptr.6858>
- Zhang, S., Kou, X., Zhao, H., Mak, K. K., Balijepalli, M. K., & Pichika, M. R. (2022). Zingiber officinale var. rubrum: Red Ginger's Medicinal Uses. *Molecules*, 27(3). <https://doi.org/10.3390/molecules27030775>
- Zivarpour, P., Nikkhah, E., Maleki Dana, P., Asemi, Z., & Hallajzadeh, J. (2021). Molecular and biological functions of gingerol as a natural effective therapeutic drug for cervical cancer. *Journal of Ovarian Research*, 14(1). <https://doi.org/10.1186/s13048-021-00789-x>